ISSN 0036-0295, Russian Metallurgy (Metally), Vol. 2013, No. 2, pp. 149–156. © Pleiades Publishing, Ltd., 2013.
Original Russian Text © V.V. Filippov, 2013, published in Rasplavy, 2013, No. 2, pp. 54–63.

Acoustic Investigations of Ga–Pb Miscibility Gap Melts

V. V. Filippov

Ural Federal University, ul. Mira 19, Yekaterinburg, 620002 Russia
e-mail: vvfilippov@mail.ru

Received November 8, 2012

Abstract—The ultrasound velocity is measured in Ga–Pb melts from the monotectic temperature to 1100 K over the entire concentration range by a pulsed-phase method. Anomalies are detected in the temperature dependences of the ultrasound velocity near the critical point. The boundary of the miscibility gap is determined from the results of acoustic measurements. The miscibility gap temperatures measured by the acoustic method agree well with the reported data.

DOI: 10.1134/S003602951302016X

INTRODUCTION

The signs of microsegregation of atoms of the same kind were detected in miscibility gap systems in the field of the single-phase state of melts. The X-ray diffraction patterns of such melts can be represented as the superposition of the X-ray diffraction patterns of the pure components [1]. Various anomalies (in particular, viscosity and electrical resistivity maxima [2]) are visible in property isotherms at temperatures insignificantly higher than the critical miscibility gap temperature near the critical concentration. The appearance of microsegregation in such systems is related to a preferred interaction of atoms of the same kind and can occur near the critical point by a fluctuation way. However, the fluctuation scale should decrease rapidly with the distance from the critical point.

The purpose of this work is to measure the ultrasound velocity in Ga–Pb melts and to determine the miscibility gap boundary for them from these measurements.

EXPERIMENTAL

Ultrasound velocity υ_s in Ga–Pb melts was measured by a pulsed-phase method. It is based on direct measurements of wavelength λ and sound frequency f and the subsequent calculation of the sound velocity by the formula

$$\upsilon_s = \lambda f. \quad (1)$$

Figure 1 shows the schematic diagram of the experimental setup. A G5-72 generator emits rectangular 1- to 5-μs electric signals at a repetition frequency of ~800 Hz, and they are filled with a high-frequency (f = 33.83 MHz) sinusoidal voltage pulses supplied from a G4-151 generator. The pulse amplitude is smoothly controlled in the range 0–10 V. Pulses are supplied to the lower emitting piezoelectric elements of measuring and reference cells, which have the same design and are connected in parallel. The working cell is preliminarily filled with a metallic melt to be studied, and the reference cell is filled with distilled water.

After passing through the measuring and reference cells, acoustic pulses are directed to the upper receiving piezoelectric elements, where they are again converted into electric pulses. Since the delay times of acoustic signals in both cells are chosen to be approximately the same, the electric pulses at their output pass through a connecting circuit and interfere with each other. The result of this interference is enhanced in a selective detector and is visible on an oscilloscope display.

The upper waveguide of the measuring cell can move along its vertical axis, and the displacement is measured by a digital micrometer with a scale interval of 0.001 mm. In this case, a sequence of interference signal extrema, which are spaced sound wavelength λ apart, are visible on the oscilloscope display.

Therefore, the sound wavelength in the melt can be calculated by the formula

$$\lambda = \Delta h/n, \quad (2)$$

where n is the number of the minima of the resulting oscillation detected on the oscilloscope display when the upper waveguide of the measuring cell travels distance Δh. Then, with allowance for Eqs. (1) and (2), the sound velocity in the melt under study is

$$\upsilon_s = (\Delta h/n)f. \quad (3)$$

This method of acoustic measurements is characterized by the possibility of measuring the local ultrasound velocity at various distances from the crucible bottom, which makes it possible to detect a macroscopic heterogeneity of the melt in height (e.g., the separation of the melt into two liquid phases). The authors of [3, 4] showed that the position of the boundary between two liquids can be determined from both an ultrasound velocity jump and a sharp decrease in the amplitude of

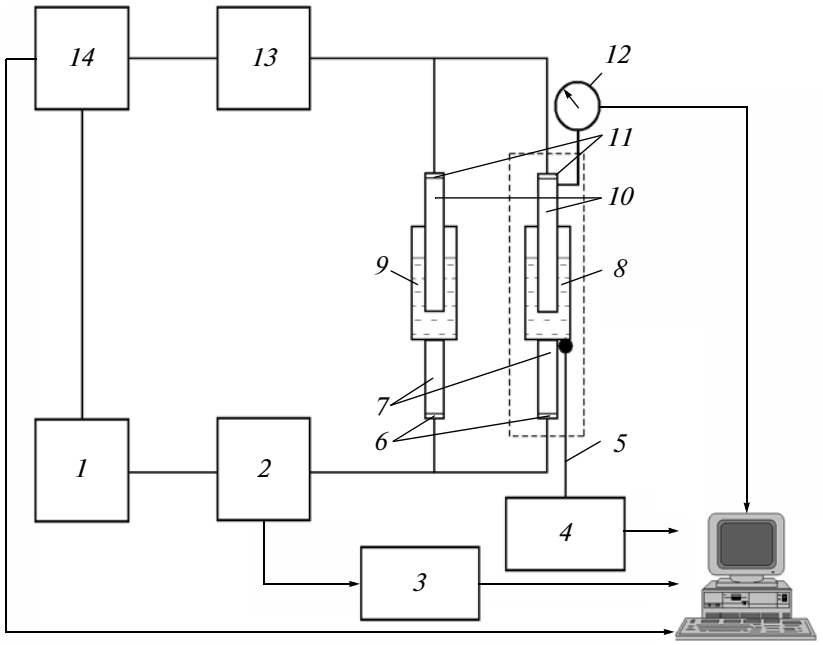

Fig. 1. Schematic diagram of the experimental setup: (*1*) pulsed-signal generator, (*2*) sinusoidal signal generator, (*3*) frequency meter, (*4*) digital voltmeter, (*5*) thermocouple, (*6*) and (*11*) piezoelectric elements, (*7*) and (*10*) waveguides, (*8*) container with a sample, (*9*) container with a reference liquid, (*12*) digital micrometer, (*13*) selective amplifier, and (*14*) digital oscilloscope.

an ultrasonic signal passing through a melt. The accuracy of determining this boundary from the ultrasonic signal amplitude is an order of magnitude higher than the accuracy of determining this boundary from the ultrasound velocity [4]. The miscibility gap temperature can be determined from the appearance or disappearance of the boundary between two liquids upon cooling or heating of a sample.

Another method of determining a miscibility gap is based on measuring the ultrasound velocity in one- and two-phase fields. We measured the temperature dependences of the ultrasound velocity in a one-phase field for alloys of various compositions and then constructed their concentration dependences. In a two-phase field, we measured temperature–concentration dependence $\upsilon_s(T, x)$ along a miscibility gap. The points of intersection of measured ultrasound velocity isotherms with curve $\upsilon_s(T, x)$ determine the coordinates of the miscibility gap for a certain temperature.

The authors of [5, 6] proposed a very sensitive and simple method of static loading to find solidus, monotectic, and eutectic points. This method can be executed using the equipment for measuring the ultrasound velocity by the pulsed-phase method. The temperature dependence of the size of the solid part of a sample h (i.e., the distance between the waveguides strongly pressed against this part) was determined in heating at a rate of 0.5–1 K/h. When a liquid phase appears at a small load applied to the upper waveguide, h decreases sharply and the phase-transition temperature can be detected accurate to 0.5 K. The temperature of the end of sample melting can be determined from the appearance of an acoustic signal [4].

The carrier frequency of acoustic vibrations (f = 33.83 MHz) was measured by an electronic frequency meter at an absolute error of ±50 Hz, which is about $\pm 2 \times 10^{-4}$% in relative units. Therefore, the error of measuring the sound wave length mainly contributes to the error of determining the ultrasound velocity. To increase the experimental accuracy, we have to increase acoustic base Δh of these measurements.

The samples were alloyed in a quartz measuring cell from gallium of 99.999 wt % purity and lead of 99.99 wt % purity. The ultrasound velocity was measured in a high-purity helium atmosphere upon cooling from 1100 K to the monotectic temperature. Every experimental point was obtained after isothermal holding of a sample for 30 min at a temperature maintained accurate to ±0.5 K. The ultrasound velocity corresponding to this temperature was averaged over 10–20 measurements at an acoustic base Δh = 3–4 mm. The random error in determining the average value did not exceed 0.3% at a systematic error of about 0.03%.

RESULTS AND DISCUSSION

We measured ultrasound velocity υ_s as a function of temperature for pure gallium, lead, and their alloys containing 10, 20, 30, 35, 38, 40, 44, 50, 60, 70, 80, and 90 at % Ga.

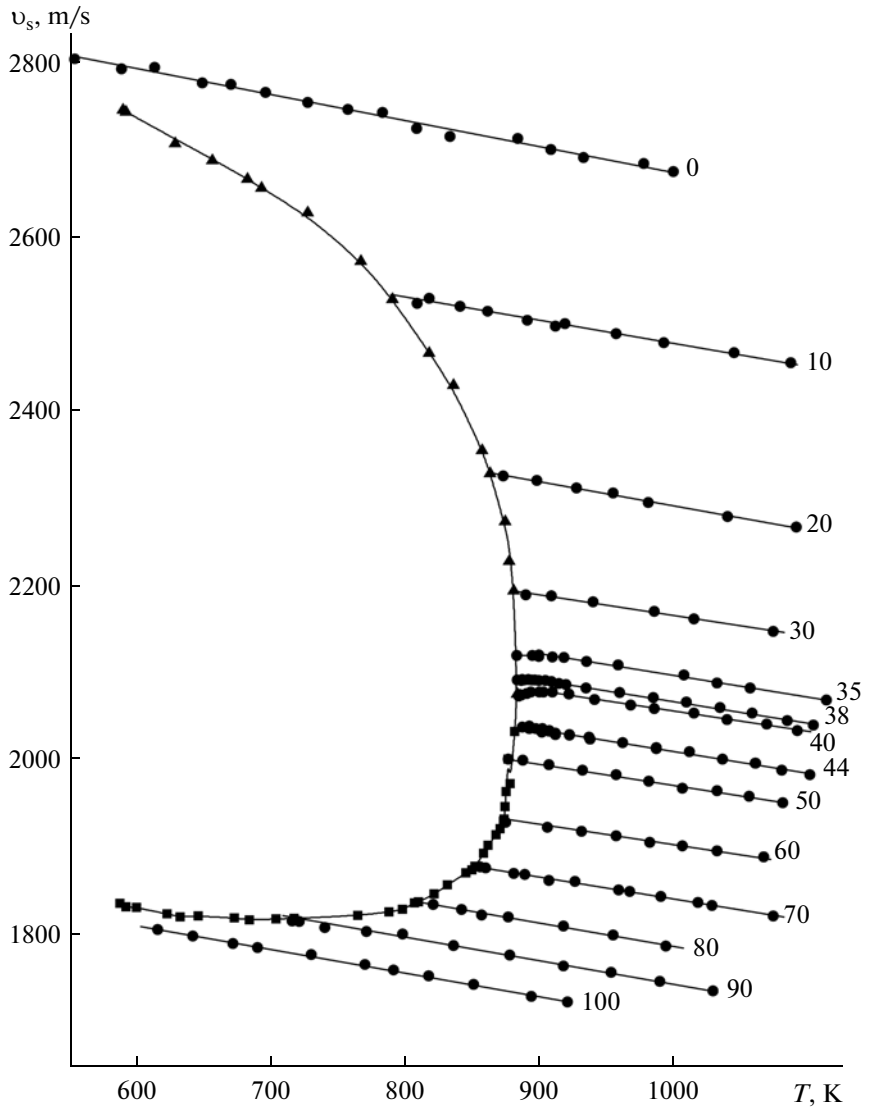

Fig. 2. Temperature dependences of the ultrasound velocity in Ga–Pd melts in (▲) gallium-rich phase, (■) lead-rich phase, and (●) single-phase field. Numerals at the curves, the lead content in an alloy (at %).

Figure 2 shows the temperature dependences of υ_s in liquid gallium–lead alloys. The ultrasound velocity increases linearly with decreasing temperature down to miscibility gap T_{mg} for all compositions under study except for the melts containing 35, 38, and 40 at % Pb, where υ_s deviates from a linear run below 910 K. This anomaly is related to the preferred interaction of atoms of the same kind near the critical point.

Table 1 gives the coefficients in the equation

$$\upsilon_s(T) = b_0 - b_1 T, \quad (4)$$

obtained by the least squares method.

Below T_{mg}, the $\upsilon_s(T)$ curve splits into two curves: the lower branch describes the ultrasound velocity in a lead-rich phase ($\upsilon_s^{"tr}$), and the upper branch, in a gallium-rich phase ($\upsilon_s^{'tr}$). When the temperature decreases further, the ultrasound velocity in the two-phase field changes along the $\upsilon_s^{'tr}$ and $\upsilon_s^{"tr}$ curves down to the monotectic temperature. The $\upsilon_s^{'tr}$ and $\upsilon_s^{"tr}$ curves limit the area of existence of two liquids in the υ_s–T diagram. The temperature at which these curve merge is the critical temperature.

The deviation of our values of υ_s from the data in [7] obtained at a frequency of 5 MHz does not exceed 0.6% over the entire temperature and concentration ranges. The exception is the melt with 40 at % Pb, in which no anomalies in the $\upsilon_s(T)$ curve near T_{mg} was observed in [7].

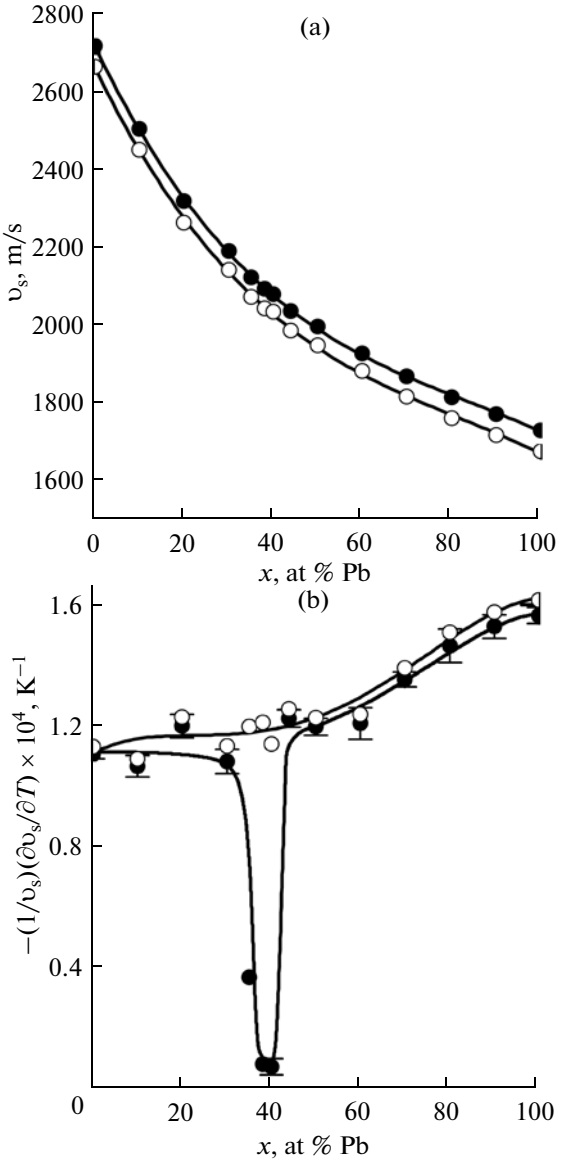

Fig. 3. (a) Concentration dependence of the ultrasound velocity and (b) its temperature coefficient for Ga–Pb melts: (●) 900 and (○) 1100 K.

Figure 3 shows the concentration dependences of ultrasound velocity υ_s and its temperature coefficient for Ga–Pb melts at 900 and 1100 K. The ultrasound velocity isotherms do not exhibit specific features, and the concentration dependences of the temperature coefficient of υ_s below 910 K has a deep minimum near 40 at % Pb. This minimum is related to the anomaly of the temperature dependence of υ_s near the critical point (Fig. 2). The depth of the minimum grows when the critical temperature T_{cr} is approached.

The data on miscibility gap boundary $T_{mg}(x)$ obtained in this work are presented in Fig. 4 and Tables 2 and 3. The miscibility gap temperatures were measured by the two methods described above. Using these methods, we determined miscibility gap boundary $T_{mg}(x)$, which is indicated by the solid line in Fig. 4. Figure 4 also shows the data from [7–13] and review [14]. The miscibility gap temperatures determined in this work agree well with the results in [7, 9–11, 14] and are substantially lower than the data obtained in [12, 13] in the region with a high lead content. The results from [8] for gallium-rich melts are lower than the other data presented in Fig. 4.

Monotectic temperature T_m was determined by the static loading (SL) method and from the appearance of an acoustic signal after melting a sample. At a relatively low heating rate (0.5–1 K/h), these methods give similar phase-transition temperatures. In the SL method, the heating rate weakly affects the measurement results, whereas the second method gives higher values of T_m at heating rates of 1 K/h or higher. Therefore, the monotectic temperature in most samples of various compositions was determined by SL method.

Table 1. Coefficients in Eq. (4), error $\delta\upsilon_s$ in determining the ultrasound velocity, and the corresponding temperature ranges of measurement

x, at % Pb	b_0, m/s	b_1, m/(s K)	$\delta\upsilon_s$, m/s	T, K
0	2934.7 ± 5.2	0.191 ± 0.015	1.6	303–380
	2973.7 ± 2.2	0.299 ± 0.004	3.4	380–1000
10	2746.3 ± 7.4	0.267 ± 0.008	2.1	787–1090
20	2571.5 ± 7.7	0.278 ± 0.008	1.4	862–1090
30	2405.9 ± 8.0	0.237 ± 0.008	1.5	879–1080
35	2348.8 ± 6.5	0.248 ± 0.007	1.3	900–1110
38	2317.8 ± 5.3	0.247 ± 0.005	1.3	907–1100
40	2295.3 ± 4.9	0.236 ± 0.005	0.9	910–1120
44	2262.7 ± 3.8	0.249 ± 0.004	1.4	885–1100
50	2213.7 ± 5.1	0.239 ± 0.005	1.0	876–1080
60	2142.0 ± 9.1	0.234 ± 0.009	1.6	872–1070
70	2097.8 ± 4.0	0.253 ± 0.004	0.9	852–1080
80	2056.6 ± 8.1	0.266 ± 0.009	1.3	808–1000
90	2017.9 ± 5.7	0.271 ± 0.006	1.6	707–1030
100	1976.7 ± 2.9	0.271 ± 0.004	1.2	601–920

Table 2. Phase compositions and the monotectic temperatures

Phase composition, at % Pb			T, K	Investigation method	Reference
L_1	L_2	(Pb)			
1.8	94	–	586	Ultrasound velocity	[7]
–	–	–	584.1	Heat capacity	[8]
2.4	94.5	–	586	DTA	[9]
2.4 ± 0.1	93.3 ± 1.0	–	586.0 ± 1.5	γ method	[10]
–	–	–	586.0 ± 0.8	Electrical resistivity	[12]
–	86.47	–	590	Thermal analysis	[15]
–	95.8	99.55	584 ± 1	Melt quenching	[16]
2.4 ± 0.1	94.6 ± 0.3	–	586 ± 1	Ultrasound velocity	This work

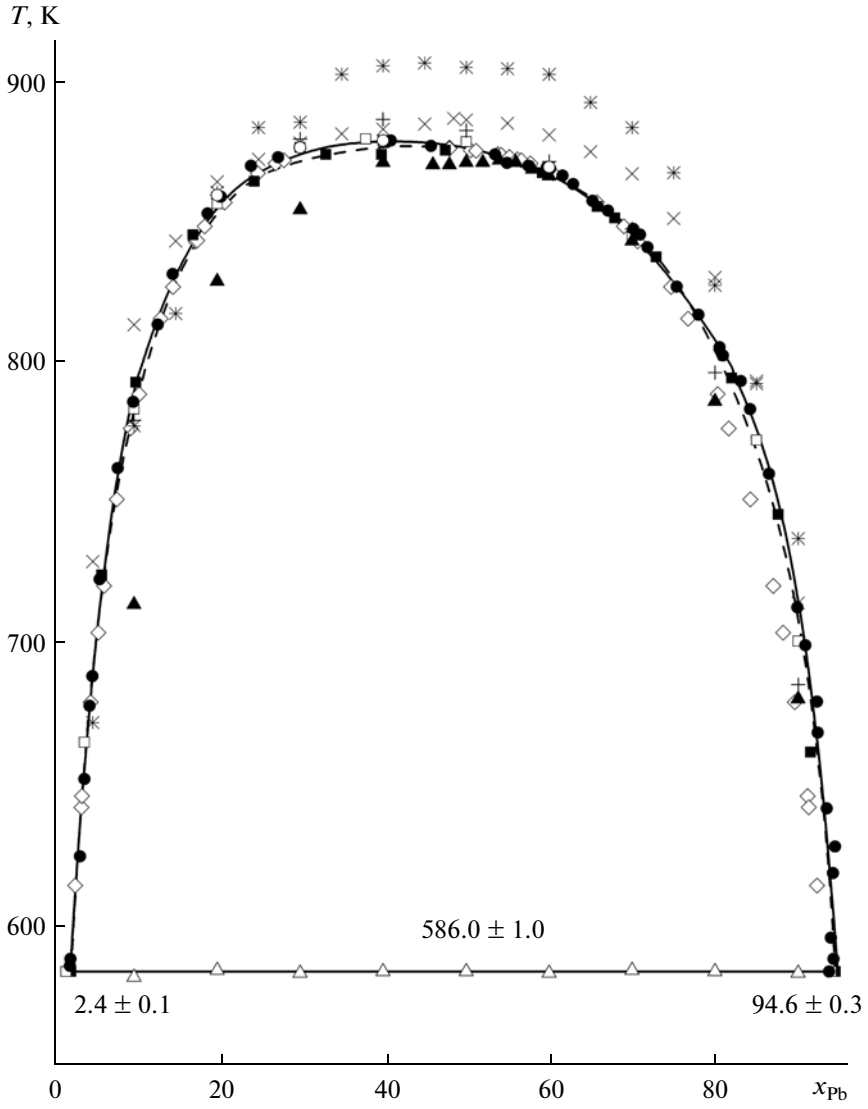

Fig. 4. Miscibility gap boundary in the Ga–Pb phase diagram constructed (○) from ultrasonic signal amplitude, (●) from the ultrasound velocity, and (△) by the SL method in comparison with the reported data: (□) [7], (▲) [8], (■) [9], (◇) [10], (+) [11], (*) [12], (X) [13], and (- - -) [14].

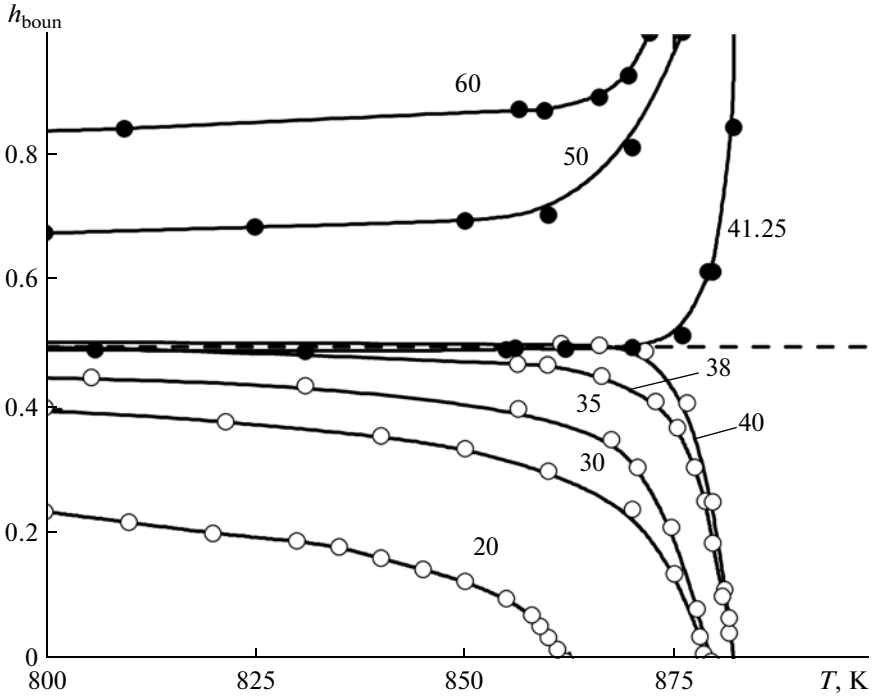

Fig. 5. Temperature dependences of the relative coordinate of the interphase boundary h_{boun} in Ga–Pb melts at (○) $x < x_{cr}$ and (●) $x > x_{cr}$. Numerals at the curves, the lead content in an alloy (at %).

Figure 5 shows the temperature dependences of the coordinate of the boundary between liquid phases h_{boun} for eight compositions. This boundary for the melts containing 20–40 at % Pb lies in the lower half of the melt ($h_{boun} < 0.5$). As the temperature increases, it shifts downward and disappears near the crucible bottom at T_{mg}. In contrast, in the melts with 41.25, 50, and 60 at % Pb, the interphase boundary is located in the upper half of the melt and shifts toward the upper level of the melt ($h_{boun} \to 1$) as the temperature increases.

To analyze these data, we express coordinate h_{boun} as a function of temperature and composition,

$$h_{boun}(x,T) = \frac{V''N''}{V'N' + V''N''} = \frac{V''(x - x')}{V'(x'' - x) + V''(x - x')}, \quad (5)$$

where x^α and V^α are the lead concentration and the molar volume of phase α (symbol α belongs to the gallium-rich (superscript ') or the lead-rich (superscript '') phase). The number of moles N' and N'' in the coexisting phases were determined from the lever rule. As follows from Eq. (5), condition $h_{boun} = 0$ is always met

Table 3. Composition (x_{cr}) and temperature (T_{cr}) of the miscibility gap critical point

x_{cr}, at % Pb	T_{cr}, K	Method of determining x_{cr}	Reference
37.9	882	From the maximum in a miscibility gap curve	[7]
~50	879	The same	[9]
41.9 ± 1.0	879.3 ± 1.5	Rectilinear diameter rule	[10]
~40	889	From the maximum in a miscibility gap curve	[11]
48.0 ± 0.5	909.0 ± 1.6	Rectilinear diameter rule	[12]
48.5	889 ± 1.3	The same	[13]
40.8 ± 0.1	881.6 ± 1.0	From the temperature depedence of the vertical coordinate of the interphase boundary	This work

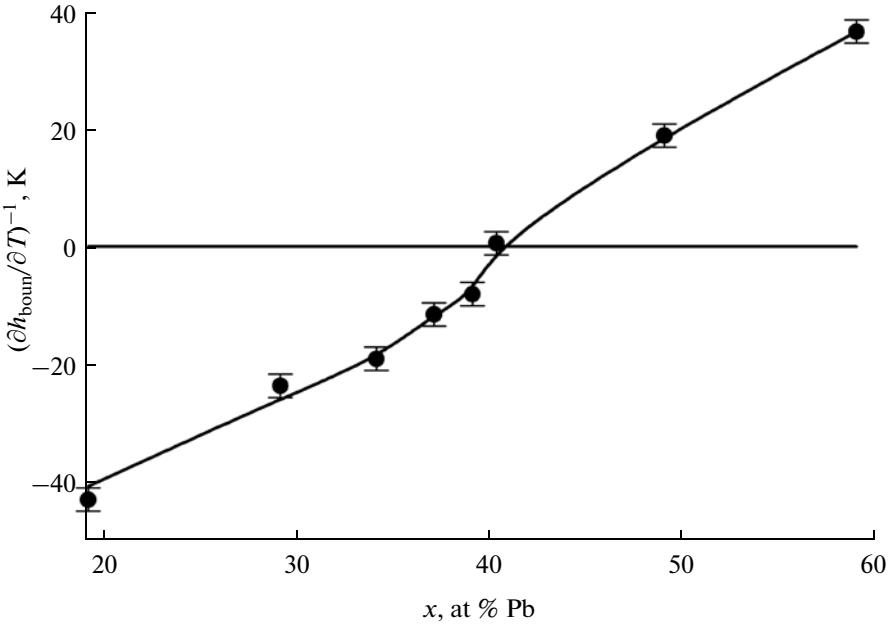

Fig. 6. Concentration dependence of the temperature derivative of interphase boundary coordinate h_{boun} along the miscibility gap curve for Ga–Pb melts.

for compositions $x < x_{cr}$ along the miscibility gap curve ($x = x'$). In contrast, if $x > x_{cr}$, we have $h_{boun} = 1$ along the miscibility gap curve ($x = x''$).

To determine the critical composition accurately, we express the temperature derivative of h_{boun} along the miscibility gap curve from Eq. (5),

$$\left(\frac{\partial h_{boun}}{\partial T}\right)'_{x=x'} = -\frac{V''}{V'}\frac{(\partial x'/\partial T)}{x'' - x'},$$
$$\left(\frac{\partial h_{boun}}{\partial T}\right)''_{x=x''} = -\frac{V'}{V''}\frac{(\partial x''/\partial T)}{x'' - x'}. \quad (6)$$

It follows from these equations that the concentration dependences of $(\partial h_{boun}/\partial T)'$ and $(\partial h_{boun}/\partial T)''$ become $-\infty$ and $+\infty$, respectively, at the critical point. In contrast to $(\partial h_{boun}/\partial T)$, the concentration dependence of $(\partial h_{boun}/\partial T)^{-1}$ is continuous and zero at the critical point. Therefore, this function can be used to determine the critical point. Figure 6 shows the concentration dependence of $(\partial h_{boun}/\partial T)^{-1}$ for a Ga–Pb melt near the critical concentration. The critical concentration found from this dependence ($x_{cr} = 40.8 \pm 0.1$ at % Pb) coincides with the value (41.9 ± 1.0 at % Pb [10]) obtained by the rectilinear diameter rule. Note that the accuracy of determining x_{cr} by this method is an order of magnitude higher than that of the rectilinear diameter rule.

Thus, the position of the miscibility gap determined in this work agrees well with the most reliable data obtained in other works. The proposed method of studying the temperature dependence of the vertical coordinate of the interphase boundary allowed us to determine x_{cr} more accurately as compared to the traditional rectilinear diameter rule.

CONCLUSIONS

Using a pulsed-phase method, we measured the temperature dependences of the ultrasound velocity in gallium, lead, and their alloys containing 10, 20, 30, 35, 38, 40, 44, 50, 60, 70, 80, and 90 at % Ga. Anomalies were detected in the temperature dependences of the ultrasound velocity near the critical point. These anomalies are related to the preferred interaction of atoms of the same kind near the critical point and are most pronounced in the concentration dependence of the temperature coefficient of the ultrasound velocity. Below 910 K this dependence has a deep minimum near the critical composition. The depth of this minimum grows when the critical temperature is approached. The miscibility gap boundary determined by the acoustic method agrees well with the reported data.

ACKNOWLEDGMENTS

This work was supported by the Presidium of the Russian Academy of Sciences, project no. 12-P-3-1032.

REFERENCES

1. A. R. Skryshevskii, *Structural Analysis of Liquids* (Vysshaya Shkola, 1971).
2. P. P. Arsent'ev and L. A. Koledov, *Metallic Melts and Their Properties* (Metallurgiya, Moscow, 1976).

3. V. V. Filippov, D. A. Yagodin, and P. S. Popel', "Acoustic method of measuring the interfacial tension at the boundary of immiscible liquids," Teplofizika Vysokikh Temperatur **47** (2), 201–206 (2009).
4. V. V. Filippov, "Acoustic investigations of the heterogeneous states of Ga–Pb melts," *Cand. Sci. (Phys.-Math.) Dissertation*, Yekaterinburg, Ural Polytechnical Institute, 2009.
5. V. G. Il'ves, V. V. Filippov, and S. P. Yatsenko, "Phase equilibria in the In–Bi–Pb system," Izv. Ross. Akad. Nauk, Ser. Met., No. 5, 166–168 (1992).
6. V. G. Il'ves, V. V. Filippov, and S. P. Yatsenko, "In_2Bi–Ga phase diagram," Izv. Ross. Akad. Nauk, Ser. Met., No. 4, 231–235 (1993).
7. A. R. Regel', V. M. Glazov, and S. G. Kim, "Acoustic Studies of the structural changes in heating of semiconductor and semimetal melts," Fiz. Tekh. Poluprovodn. **20** (8), 1353–1375 (1986).
8. M. Mathon, J. M. Miane, P. Gaune, et al., "Gallium + lead system: molar heat capacity and miscibility gap," J. Alloys and Compounds **237**, 155–164 (1996).
9. B. Predel, "Zustandsbilder gallium–blei und gallium–thallium," Z. Metallkd. **50** (4), 663–667 (1959).
10. R. A. Khairulin and S. V. Stankus, "Application of a γ attenuation technique for the study of phase equilibria in binary liquid systems with a miscibility gap," High Temperatures–High Pressures **32** (2), 193–198 (2000).
11. A. Ben Abdellah, J. G. Gasser, A. Makradi, et al., "Resistivity of the liquid gallium–lead miscibility gap system," Phys. Rev. B **68**, 184201 (2003).
12. B. Sokolovskii, Yu. Plevachuk, and V. Didoukh, "Electroconductivity and liquid–liquid equilibrium in the Pb–Ga system," Phys. Stat. Sol. (a) **148**, 123–128 (1995).
13. Yu. O. Plevanchuk, V. M. Sklyarchuk, O. D. Alekhin, and L. A. Bulavin, "Viscosity of Ga–Pb melts with a miscibility gap," Zh. Fizicheskikh Dostizhenii **9** (4), 333–335 (2005).
14. T. B. Massalski, *Binary Alloy Phase Diagrams* (Metals Park, Ohio, 1990).
15. N. A. Pushin, S. Stepanovic, and V. Stajic, "On the Ga-alloys with Zn, Cd, Hg, Sn, Pb, Bi, and Al," Z. Anorg. Chem **209**, 329–334 (1932).
16. J. N. Greenwood, "The solid solutions of gallium in lead," J. Inst. Met. **87**, 91–93 (1958/59).

Translated by K. Shakhlevich